

A possible origin of the Galactic Center magnetar SGR 1745–2900

Quan Cheng¹, Shuang-Nan Zhang¹ and Xiao-Ping Zheng²

¹ Key Laboratory of Particle Astrophysics, Institute of High Energy Physics, Chinese Academy of Sciences, Beijing 100049, China; qcheng@ihep.ac.cn

² Institute of Astrophysics, Central China Normal University, Wuhan 430079, China

Received 2016 November 6; accepted 2017 February 25

Abstract Since there is a large population of massive O/B stars and putative neutron stars (NSs) located in the vicinity of the Galactic Center (GC), intermediate-mass X-ray binaries (IMXBs) constituted by an NS and a B-type star probably exist there. We investigate the evolutions of accreting NSs in IMXBs (similar to M82 X-2) with a $\sim 5.2 M_{\odot}$ companion and orbital period $\simeq 2.53$ d. By adopting a mildly super-Eddington rate $\dot{M} = 6 \times 10^{-8} M_{\odot} \text{ yr}^{-1}$ for the early Case B Roche-lobe overflow (RLOF) accretion, we find that only in accreting NSs with quite elastic crusts (slippage factor $s = 0.05$) can the toroidal magnetic fields be amplified within 1 Myr, which is assumed to be the longest duration of the RLOF. These IMXBs will evolve into NS+white dwarf (WD) binaries if they are dynamically stable. However, before the formation of NS+WD binaries, the high stellar density in the GC will probably lead to frequent encounters between the NS+evolved star binaries (in post-early Case B mass transfer phase) and NSs or exchange encounters with other stars, which may produce single NSs. These NSs will evolve into magnetars when the amplified poloidal magnetic fields diffuse out to the NS surfaces. Consequently, our results provide a possible explanation for the origin of the GC magnetar SGR 1745–2900. Moreover, the accreting NSs with $s > 0.05$ will evolve into millisecond pulsars (MSPs). Therefore, our model reveals that the GC magnetars and MSPs could both originate from a special kind of IMXB.

Key words: stars: neutron — stars: magnetars — stars: magnetic field — pulsars: individual (SGR 1745–2900)

1 INTRODUCTION

Magnetars are generally regarded as strongly magnetized neutron stars (NSs). Release of their magnetic energy could power the burst activities of soft gamma-ray repeaters and/or anomalous X-ray emissions of some pulsars (Thompson & Duncan 1995, 1996). Moreover, the plateau afterglows of some gamma-ray bursts (GRBs), as well as the light curves of superluminous supernovae and bright mergernovae, can be well understood in the magnetar scenario, which suggests that the central objects are newly born, millisecond rotating magnetars with surface dipole magnetic fields $B_s = 10^{14} - 10^{15}$ G (e.g., Dai & Lu 1998; Zhang & Mészáros 2001; Fan & Xu 2006; Kasen & Bildsten 2010; Yu et al. 2010; Dall’Osso et al. 2011; Rowlinson et al. 2013; Yu et al. 2013; Lü et al. 2015). Unlike GRB magnetars, Galactic magnetars have relatively long spin periods (2–12 s) and a wide dipole

magnetic field distribution, ranging from 6×10^{12} G to 2×10^{15} G (Olausen & Kaspi 2014). Even though SGR 0418+5729 and Swift J1822.3–1606 both have much lower dipolar fields of 6×10^{12} G and 1.35×10^{13} G, respectively (Rea et al. 2013c; Scholz et al. 2014), strong initial surface dipole and internal toroidal magnetic fields of $\sim 10^{14}$ G and $\sim 10^{15} - 10^{16}$ G are required to recover the observed properties of the two magnetars (Turolla et al. 2011; Rea et al. 2012).

To date, 28 magnetars have been discovered: 26 in the Galaxy, one in the Large Magellanic Cloud and one in the Small Magellanic Cloud¹. For the Galactic magnetars, more than half of them are located in the inner Galaxy (Olausen & Kaspi 2014). The most striking one is SGR 1745–2900, which has a projected offset of only 0.12 pc from the Galactic Center (GC) black

¹ <http://www.physics.mcgill.ca/~pulsar/magnetar/main.html>

hole, Sgr A* (Rea et al. 2013b). SGR 1745–2900 was first discovered by *Swift* XRT when it underwent an X-ray outburst (Kennea et al. 2013). This source was identified as a magnetar after the discovery of its 3.76 s pulsations by *NuSTAR* (Mori et al. 2013). Meanwhile, the spin-down rate of this magnetar is determined to be $\dot{P} = 6.61 \times 10^{-12} \text{ s s}^{-1}$, which gives a surface equatorial dipole magnetic field of $1.6 \times 10^{14} \text{ G}$ via $B_d = 3.2 \times 10^{19} \sqrt{P\dot{P}}$ (Rea et al. 2013a). Subsequently, through a 4 month observation using *NuSTAR* and *Swift* after its discovery, Kaspi et al. (2014) found that the spin-down rate of SGR 1745–2900 increased by about 2.6 times, which yields a stronger dipole field of $2.3 \times 10^{14} \text{ G}$. Follow-up radio observations also detected this GC magnetar using the Effelsberg Radio Telescope, the Nançay Radio Telescope, the Very Large Array, Jodrell Bank, the Australia Telescope Compact Array, the Green Bank Telescope and the Parkes Radio Telescope (Eatough et al. 2013; Rea et al. 2013a; Shannon & Johnston 2013), making it the fourth radio-magnetar found in the Galaxy. Most surprisingly, Spitler et al. (2014) suggested that the pulsed emission from this magnetar could even be detected at frequencies down to 1.2 GHz, which indicates that the pulse profile broadening due to scattering material at the GC may be much weaker than previously predicted. As a result, if scattering that occurs in the whole GC region is indeed much weaker, many canonical and millisecond pulsars (MSPs) should have been detected by previous surveys (Spitler et al. 2014), since ~ 1000 radio pulsars are predicted to orbit Sgr A* with periods less than 100 yr (Pfahl & Loeb 2004). However, no normal pulsars have been detected within the central parsec of Sgr A* through several surveys at different observing frequencies (Johnston et al. 1995; Johnston et al. 2006; Deneva et al. 2009; Macquart et al. 2010; Bates et al. 2011).

Many reasons may be responsible for the lack of detection of GC pulsars: spatially complex scattering (Spitler et al. 2014), intrinsic deficit of pulsars (Spitler et al. 2014) and MSPs dominating the pulsar population which have not been found by previous GC pulsar searches (Macquart & Kanekar 2015). Specifically, the intrinsic deficit of pulsars may result from dark matter accretion-induced collapse of GC NSs (Fuller & Ott 2015), or efficient formation of magnetars rather than ordinary pulsars in the GC as implied by the discovery of SGR 1745–2900 (Dexter & O’Leary 2014). Since a large amount of massive and strongly magnetized O/B stars exist in the GC, their collapses could efficiently produce magnetars, which spin down very rapidly (Dexter & O’Leary 2014). Moreover, a large number of MSPs are

suggested to exist in the GC due to the very dense stellar environment (Spitler et al. 2014; Dexter & O’Leary 2014; Macquart & Kanekar 2015).

Inspired by this suggestion, we propose that the GC is indeed a region that is very efficient for magnetar formation. However, these magnetars could originate from the NSs in intermediate-mass X-ray binaries (IMXBs) comprised of an NS and a massive B-type star². The predicted large population of NSs in combination with a large amount of massive B-type stars will reasonably result in many IMXBs in the GC. Specifically, we consider the evolutions of accreting NSs in a special kind of IMXB, of which the companions are evolved stars with mass $M_c \sim 5.2 M_\odot$, and orbital period $P_{\text{orbit}} \simeq 2.53 \text{ d}$. In such an IMXB system, Roche-lobe overflow (RLOF) accretion could take place at the end of the main sequence of the massive companion when it starts to expand (namely the Hertzsprung gap phase) (Karino & Miller 2016). The early Case B RLOF accretion proceeds on a thermal timescale with a high accretion rate, which may be responsible for the high observed X-ray luminosity of the ultraluminous X-ray source (ULX) M82 X-2 (Bachetti et al. 2014; Dall’Osso et al. 2015; Karino & Miller 2016). The RLOF accretion timescale is some fraction of the time that the companion remains in the Hertzsprung gap phase. For a $5.2 M_\odot$ companion, the duration of the Hertzsprung gap phase is about 1.5 Myr (Karino & Miller 2016). To accurately determine the timescale of RLOF accretion, one needs to perform a detailed stellar evolution calculation (Karino & Miller 2016), which is beyond the scope of this paper. We assume that the longest duration of RLOF accretion is 1 Myr. Actually, if the accretion rate is much higher (than the Eddington limit \dot{M}_{Edd}), within 1 Myr the NS can be spun up to the critical frequency to trigger the r -mode. Thus, a shorter RLOF accretion timescale will not change our result qualitatively.

When RLOF accretion commences in an IMXB, the NS, which is initially not in spin equilibrium, will be spun up. The accreting NS may be observed as a ULX similar to M82 X-2. The high accretion rate and sufficiently long duration of the RLOF accretion in such a binary system could easily spin up the NS to millisecond period if its dipole magnetic field is $10^8 - 10^9 \text{ G}$ as suggested in Kluźniak & Lasota (2015). The subsequent evolution of the NS depends on its properties and the accretion rate. If the spin equilibrium frequency ν_{eq} is higher

² The B-type stars usually have masses in the range $2.1 M_\odot - 16 M_\odot$ (Habets & Heintze 1981), thus they have relatively long main-sequence lifetimes of $10^7 - 1.6 \times 10^9 \text{ yr}$ (Bhattacharya & van den Heuvel 1991)

than the critical frequency ν_{cr} at which r -mode arises, the accreting NS will succumb to r -mode instability when ν_{cr} is reached (Cuofano & Drago 2010; Cuofano et al. 2012). The r -mode-induced differential rotation could produce a strong internal toroidal magnetic field, which will subsequently experience Tayler instability, leading to the formation of an enhanced poloidal magnetic field (Cheng & Yu 2014). Through such a dynamo process, the accreting NS could evolve into an NS with high internal toroidal and poloidal magnetic fields. However, if $\nu_{\text{eq}} < \nu_{\text{cr}}$, the accreting NS will evolve into a millisecond rotating NS without enhanced internal magnetic fields since r -mode could never arise.

Evolution of such an IMXB is still an open issue. It is possible that delayed dynamical instability will set in after the early Case B mass transfer due to the large mass ratio between the companion and the NS (Bhattacharya & van den Heuvel 1991; Tauris et al. 2000; Shao & Li 2012, 2015). The IMXB will experience common envelope evolution (CEE), possibly resulting in a merger of the binary. On the other hand, CEE is not inevitable even when rapid mass transfer onto the NS occurs as suggested by King & Ritter (1999). In this dynamically stable case, the IMXB will finally evolve into an NS binary made of an NS and a white dwarf (WD). Before the NS+WD system is finally formed, the NS can still accrete from the evolved companion after the early Case B mass transfer phase (see e.g., Tauris et al. 2000). However, the high stellar density in the GC³ could easily lead to frequent encounters between the NS+evolved star binary (in post-early Case B mass transfer phase) and NSs or exchange encounters, which may disrupt the binary system and produce a single NS (see e.g., Sigurdsson & Phinney 1995; Ivanova et al. 2008; Verbunt & Freire 2014). The scenarios were also invoked by Verbunt & Freire (2014) to account for the production of isolated pulsars in some globular clusters. Without further accretion onto the NS, the enhanced poloidal magnetic field could diffuse out to the NS surface and change the NS into a magnetar. Hence, when the magnetar is formed, it should not be in a binary in order to avoid further large amount of accretion ($\sim 0.1 M_{\odot}$ is possible) (Pan et al. 2013), which may lead to substantial decay of the magnetic field (Zhang & Kojima 2006). Our scenario provides another possible explanation for the origin of the GC magnetar SGR 1745–2900, and suggests that both the GC magnetars and MSPs could originate from IMXBs.

We note that, in principal, in order to accurately model the evolution of the accreting NS in an IMXB,

³ The stellar density in the GC is much higher than that in globular cluster cores (see e.g., Macquart & Kanekar 2015).

one should perform detailed binary evolution calculations. However, we are mainly concerned with the total amount of angular momentum carried by the accreted material that would spin up the NS to millisecond period. Hence, for simplicity, we only consider the early Case B RLOF accretion phase and assume that the NS accretes material from its surrounding Keplerian disk at a time-averaged rate $\dot{M} \gtrsim \dot{M}_{\text{Edd}}$. The assumption overestimates the accretion timescale needed to spin up the NS to millisecond period, because the accretion rate can actually be extremely super-Eddington as in the case of M82 X-2 (Kluźniak & Lasota 2015).

Our work is based on the magnetar formation mechanism of Cheng & Yu (2014). We suggest the readers refer to that paper for a detailed description of the formation process of newly born magnetars.

This paper is organized as follows. In Section 2, we present evolutions of r -mode, spin and magnetic fields of the accreting NSs in the special kind of IMXBs introduced above. Results are shown in Section 3. Finally, conclusions and discussions are presented in Section 4.

2 MODEL

During the accretion phase, the maximum spin frequency that the accreting NS could reach is the spin equilibrium frequency ν_{eq} , which is determined by setting $r_{\text{co}} \simeq r_{\text{m}}$ with r_{co} and r_{m} representing the co-rotation and magnetospheric radius, respectively. The ν_{eq} of an accreting NS with mass $M = 1.4 M_{\odot}$ and radius $R = 12.53 \text{ km}$ is (Alpar et al. 1982)

$$\nu_{\text{eq}} \simeq 3.64 \times 10^2 \left(\frac{B_{\text{d}}}{10^9 \text{ G}} \right)^{-6/7} \times \left(\frac{\dot{M}}{10^{-8} M_{\odot} \text{ yr}^{-1}} \right)^{3/7} \text{ Hz}, \quad (1)$$

where B_{d} and \dot{M} are the surface equatorial dipole magnetic field and time-averaged accretion rate of the NS, respectively. However, with the spin-up of the accreting NS, r -mode, which arises due to the action of Coriolis force (Andersson 1998; Friedman & Morsink 1998), will become unstable if the star reaches the critical frequency ν_{cr} . Consequently, the occurrence of r -mode instability requires $\nu_{\text{cr}} < \nu_{\text{eq}}$. The critical frequency ν_{cr} is determined via

$$\frac{1}{\tau_{\text{g,r}}} - \frac{1}{\tau_{\text{v}}} = 0, \quad (2)$$

where $\tau_{\text{g,r}} = 3.26(\Omega/\sqrt{\pi G \bar{\rho}})^{-6}$ is the timescale of the r -mode-induced gravitational wave (GW) emission with $\bar{\rho}$ the mean density of the star. $\tau_{\text{v}} = (\tau_{\text{bv}}^{-1} + \tau_{\text{sv}}^{-1} + \tau_{\text{vbl}}^{-1})^{-1}$

is the viscous damping timescale, where the timescales τ_{bv} , τ_{sv} and τ_{vbl} correspond to the bulk viscosity, shear viscosity and dissipation in the viscous boundary layer at the crust-core interface, respectively. The specific expressions of τ_{bv} and τ_{sv} can be found in Yu et al. (2009), while $\tau_{\text{vbl}} = 23.3 s^{-2} (\Omega / \sqrt{\pi G \bar{\rho}})^{-1/2} (T / 10^8 \text{ K})$ with T denoting the stellar internal temperature and s the slippage factor (Lindblom et al. 2000), whose value lies in the range $0.05 \lesssim s \lesssim 1$ (Levin & Ushomirsky 2001). The smaller s is, a more elastic crust the accreting NS will have. For an accreting NS with typical temperature $T \sim 10^8 \text{ K}$ (Cuofano et al. 2012; Haskell et al. 2012), the viscous damping is dominated by dissipation in the viscous boundary layer. Hence, following Equation (2), the expression for ν_{cr} is

$$\nu_{\text{cr}} \simeq 936.80 \left(\frac{T}{10^8 \text{ K}} \right)^{-2/11} s^{4/11} \text{ Hz.} \quad (3)$$

R -mode in an NS will unavoidably lead to differential rotation, which can not only determine the saturation amplitude of the mode (Sá & Tomé 2005), but also wind up the initial poloidal magnetic field to form a toroidal magnetic field (Rezzolla et al. 2000). Overall, the growth of r -mode can be increased through gravitational radiation back-reaction; however, in the meanwhile, it can also be suppressed by viscous damping, and by forming the toroidal magnetic field. In an accreting NS with a Keplerian disk, the total stellar angular momentum can be increased by angular momentum transfer from the accretion material. However, the magnetic dipole radiation (MDR) and GW emissions of the NS can decrease the total stellar angular momentum. Specifically, the GW emissions are mainly contributed by r -mode and quadrupole deformation induced by the newly formed strong toroidal magnetic field. Following Cheng & Yu (2014) and Cuofano & Drago (2010), the evolution equations for the r -mode amplitude α and angular frequency Ω of the accreting NS can be expressed as

$$\begin{aligned} \frac{d\alpha}{dt} &= \left[1 + \frac{2\alpha^2}{15}(\delta + 2) \right] \frac{\alpha}{\tau_{\text{g,r}}} - \left[1 + \frac{\alpha^2}{30}(4\delta + 5) \right] \\ &\quad \times \left(\frac{\alpha}{\tau_{\text{v}}} + \frac{\alpha}{\tau_{\text{t}}} \right) + \frac{\alpha}{2\tau_{\text{g,t}}} + \frac{\alpha}{2\tau_{\text{d}}} - \frac{\alpha \dot{M}}{2\tilde{I}\Omega} \\ &\quad \times \left(\frac{G}{MR^3} \right)^{1/2}, \quad (4) \\ \frac{d\Omega}{dt} &= -\frac{4\alpha^2\Omega}{15}(\delta + 2) \\ &\quad \times \left[\frac{1}{\tau_{\text{g,r}}} - \frac{(4\delta + 5)}{4(\delta + 2)} \left(\frac{1}{\tau_{\text{v}}} + \frac{1}{\tau_{\text{t}}} \right) \right] \end{aligned}$$

$$-\frac{\Omega}{\tau_{\text{g,t}}} - \frac{\Omega}{\tau_{\text{d}}} - \Omega \frac{\dot{M}}{M} + \frac{\dot{M}}{\tilde{I}} \left(\frac{G}{MR^3} \right)^{1/2}, \quad (5)$$

where $\tilde{I} = 0.261$ and δ denotes the initial amount of differential rotation. $\tau_{\text{d}} = 3Ic^3/(2B_{\text{d}}^2 R^6 \Omega^2)$ is the MDR timescale with $I = 0.261MR^2$ representing the moment of inertia of the NS. Moreover, strong toroidal magnetic field with volume-averaged strength \bar{B}_{t} could deform the star into a prolate ellipsoid, whose ellipticity is $\epsilon = -5\bar{B}_{\text{t}}^2 R^4 / 6GM^2$ (Cutler 2002). Hence, the GW emission timescale of the magnetically-induced deformation is $\tau_{\text{g,t}} = 5c^5 / (32GI\epsilon^2\Omega^4)$ (Cutler & Jones 2001). Following Cheng & Yu (2014), after choosing an initial internal dipolar magnetic field $B_{\text{ini}} = B_{\text{d}}(R/r)^3(2\cos\theta\mathbf{e}_r + \sin\theta\mathbf{e}_\theta)$, the growth rate of toroidal magnetic field energy is derived as

$$\frac{dE_{\text{t}}}{dt} = \frac{75}{448\pi^2} B_{\text{d}}^2 R^3 (2\delta + 3)^2 \alpha^2 \Omega \int_0^t \alpha^2 \Omega dt'. \quad (6)$$

Hence, the toroidal magnetic formation timescale can be written as (Cheng & Yu 2014)

$$\tau_{\text{t}} = \frac{448\pi^2(4\delta + 9)I^*\Omega}{75B_{\text{d}}^2 R^3 (2\delta + 3)^2 \int_0^t \alpha^2 \Omega dt'}, \quad (7)$$

where $I^* = 1.635 \times 10^{-2} MR^2$ is an effective moment of inertia for r -mode. Moreover, the toroidal magnetic field \bar{B}_{t} at the time t can be calculated as (Cheng & Yu 2014)

$$\bar{B}_{\text{t}} = \frac{15}{8\sqrt{7}\pi} B_{\text{d}}(2\delta + 3) \int_0^t \alpha^2 \Omega dt'. \quad (8)$$

A strong toroidal field will be subject to current-driven instabilities, e.g., Tayler instability. However, the growth rate of modes of Tayler instability is mainly determined by the toroidal field configuration, thermal conductivity, stratification and rotation, while the latter two effects can lead to suppression of the instability (Bonanno & Urpin 2012, 2013a,b). Moreover, the growth rate of unstable modes decreases with the increase of latitude (Bonanno & Urpin 2012, 2013a,b). If one takes $B_{\text{t}} \propto r^2$ for the toroidal field⁴, at the equator of the star, the growth of modes can only be substantially reduced but never be entirely suppressed in the presence of strong stratification, fast rotation and thermal conductivity (Bonanno & Urpin 2012, 2013a,b). The reduction of the growth rate in Tayler's modes will postpone the

⁴ By adopting equation (7) of Cuofano & Drago (2010) for the initial dipole magnetic field, the toroidal field has the form $B_{\text{t}} \propto r^2$ in most part of the stellar interior. However, in order to simplify the calculation, the above expression $B_{\text{ini}} \propto r^{-3}$ for initial dipolar field is adopted, thus $B_{\text{t}} \propto r^{-1}$. In fact, the equilibrium strengths of the amplified toroidal and poloidal fields are essentially not very sensitive to the initial dipolar field configuration that one chooses as also suggested in Cuofano & Drago (2010).

occurrence of Tayler instability, leading to a delay in amplification of the poloidal field. Unfortunately, at present we cannot quantitatively estimate the delay timescale or its effect on the evolutions of NSs. Following the numerical simulation of Braithwaite (2006), we qualitatively assume that Tayler instability will set in if the condition $\omega_A = \bar{B}_t / (R\sqrt{4\pi\rho}) > \Omega$ is satisfied with ω_A being the Alfvén frequency. With the growth of \bar{B}_t , the NS spins down through r -mode-induced and magnetic deformation-induced GW emissions. This can naturally result in $\omega_A > \Omega$. Generation of a newly enhanced poloidal field due to Tayler instability will close the dynamo loop. Finally, a poloidal-toroidal twisted torus magnetic field configuration can be formed in the NS interior. When there is no further accretion on to the NS (after disruption of the binary), the enhanced poloidal field could partially diffuse out to the surface to enhance the exterior dipolar magnetic field because of Ohmic dissipation and Hall drift. The diffusion timescale can be roughly estimated as $\tau_{\text{dif}} \simeq \tau_{\text{Hall}} \simeq 5 \times 10^6$ yr, if one takes poloidal field $B_{\text{pol}} = 10^{14}$ G and crust thickness $L = 1$ km (Goldreich & Reisenegger 1992). This suggests that if accretion is terminated before Tayler instability arises, the amplification of the surface dipole field should be delayed by $\sim 5 \times 10^6$ yr with respect to the occurrence of Tayler instability. Otherwise, the dipole field will be amplified after $\sim 5 \times 10^6$ yr since the termination of accretion. The strength of the amplified dipole field is determined by assuming a simple relation $B_d = \xi \bar{B}_t$ (with $\xi = 0.01$) (see Cheng & Yu (2014) for a detailed discussion).

Finally, the internal temperature T of the accreting NS is determined by the thermal evolution equation below

$$C_v \frac{dT}{dt} = -L_\nu - L_\gamma + H_{sv} + H_{acc}, \quad (9)$$

where C_v , L_ν , L_γ , H_{sv} and H_{acc} are the thermal capacity, neutrino luminosity, surface photon luminosity, heating due to shear viscous dissipation of r -mode and accretion heating of the star, respectively. The expressions for the first four quantities can be found in Yu et al. (2009), while the last one is the same as in Cuofano & Drago (2010).

3 RESULTS

Combining Equations (4), (5), (8) and (9) we can obtain the evolutions of r -modes, spin frequencies and magnetic fields of the accreting NSs. The initial amount of differential rotation δ is taken to be the same as in Cheng & Yu (2014). Since the results are insensitive to the initial

value of α (Cheng & Yu 2014), we fix $\alpha_i = 10^{-10}$. The initial temperature is chosen to be $T_i = 10^8$ K, which represents the typical value for accreting NSs (Cuofano et al. 2012; Haskell et al. 2012). Since we focus on evolutions of accreting NSs similar to M82 X-2, we regard the present spin period and magnetic field of M82 X-2 as the initial spin periods and dipole magnetic fields for these NSs. Thus the initial spin periods are set to be $P_i = 1.37$ s, while the initial dipole magnetic fields are selected to be $B_{d,i} = 10^8$ and 10^9 G, respectively, which approximate the strength of M82 X-2, as suggested in Kluźniak & Lasota (2015). These values may represent the post-decay strengths of the dipole magnetic field. The longest duration of early Case B RLOF accretion is assumed to be 1 Myr (see Sect. 1), whose rate is adopted to be $\dot{M} = 6 \times 10^{-8} M_\odot \text{ yr}^{-1} \simeq 3.2 \dot{M}_{\text{Edd}}$.

Figure 1 shows the evolutions of α , $\nu = (\Omega/2\pi)$, \bar{B}_t and B_d for accreting NSs with $B_{d,i} = 10^9$ G, while their s varies.

As shown in Figure 1, for the assumed accretion rate and timescale, the maximum spin frequencies that the accreting NSs with $B_{d,i} = 10^9$ G and $P_i = 1.37$ s can reach are $\simeq 246$ Hz. Similar results were also obtained in Kluźniak & Lasota (2015), which suggested that M82 X-2 may be spun up to millisecond periods. However, only the accreting NSs with fairly small s ($= 0.05$) can reach ν_{cr} and trigger r -mode instabilities within 1 Myr. Since the internal temperature when thermal equilibrium ($L_\nu = H_{acc}$) is achieved can be determined to be $T \simeq 3.9 \times 10^8$ K, the critical frequency obtained using Equation (3) is thus $\nu_{\text{cr}} \simeq 246$ Hz for $s = 0.05$ and 674 Hz for $s = 0.8$. Hence, accreting NSs with large s ($= 0.8$) will evolve into millisecond rotating NSs without r -modes when RLOF accretion is terminated. It should be mentioned that the maximum critical frequency is $\simeq 731$ Hz for $s \simeq 1$, which is still higher than that of the fastest spinning pulsar observed to date (Hessels et al. 2006). However from Equation (1), one has $\nu_{\text{eq}} (\simeq 784 \text{ Hz}) > \nu_{\text{cr}}$ for this set of $B_{d,i}$ and \dot{M} . Consequently, the maximum spin frequency allowed by our model is about 731 Hz, and if the accretion timescale is long enough, the accreting NSs could reach this value theoretically. We also note that the spin evolutions of accreting NSs in IMXBs considered here are different from those of the NSs in standard high-mass X-ray binaries (HMXBs) (Urpin et al. 1998). Their various evolution behaviors are mainly due to (i) different $B_{d,i}$ taken; (ii) different accretion modes considered (RLOF accretion versus wind accretion/propeller effect).

As r -mode grows and becomes saturated, the toroidal magnetic field is rapidly amplified to \sim

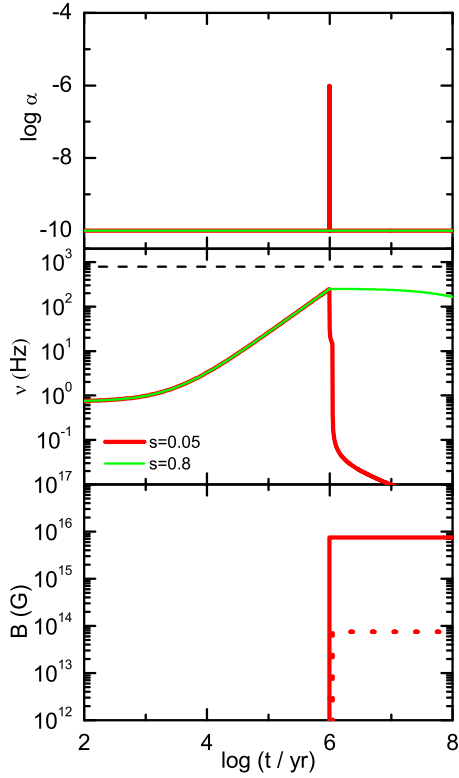


Fig. 1 Evolutions of the r -mode amplitudes (*top panel*), spin frequencies (*middle panel*) and strengths of the magnetic fields (*bottom panel*) for accreting NSs with different slippage factors s , as shown in the legends. The initial dipolar magnetic fields of the NSs are selected to be $B_{d,i} = 10^9$ G. The red solid and dotted lines in the bottom panel represent the internal toroidal and surface dipolar magnetic fields, respectively. The spin equilibrium frequency for accreting NSs with $B_{d,i} = 10^9$ G, $\dot{M} = 6 \times 10^{-8} M_{\odot} \text{ yr}^{-1}$ (black dashed line) is presented in the middle panel.

10^{16} G due to r -mode-induced differential rotation. Subsequently, the accreting NS spins down through r -mode and magnetic deformation induced GW emissions. Meanwhile, with the growth of \bar{B}_t , the Tayler instability will arise and then lead to the formation of enhanced poloidal magnetic field. After the disruption of the NS+evolved star binary (in post-early Case B mass transfer phase) due to its frequent encounters with NSs or exchange encounters with other stars (Sigurdsson & Phinney 1995; Ivanova et al. 2008; Verbunt & Freire 2014), accretion onto the NS will be completely terminated. Hence, the enhanced poloidal field could emerge at the stellar surface and amplify the surface dipole magnetic field to $\sim 10^{14}$ G. Eventually, the accreting NS could evolve into a magnetar with $B_d \sim 10^{14}$ G and $\bar{B}_t \sim 10^{16}$ G. After its formation, the magnetar rapidly spins down through magnetically-induced GW emission

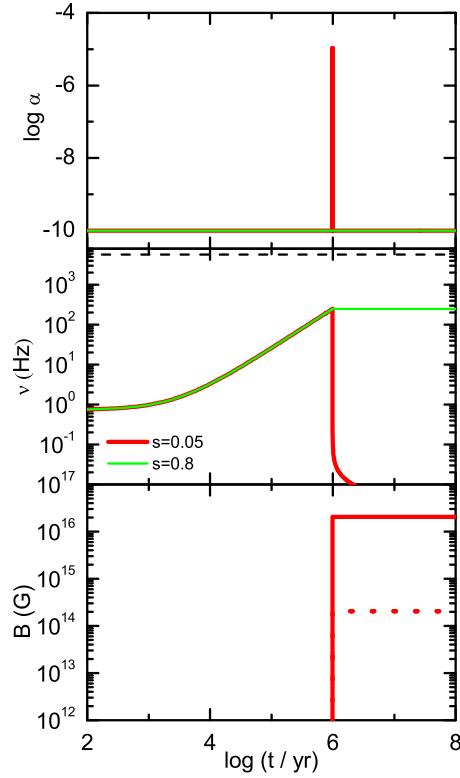


Fig. 2 Same as Fig. 1, but $B_{d,i} = 10^8$ G is taken. The black dashed line represents the spin equilibrium frequency for accreting NSs with $B_{d,i} = 10^8$ G and $\dot{M} = 6 \times 10^{-8} M_{\odot} \text{ yr}^{-1}$.

and MDR. This magnetar formation scenario is actually an extrapolation of Cheng & Yu (2014). However, there is also one obvious difference: in this work the magnetars could stem from accreting NSs with relatively large P_i (~ 1 s), whereas in Cheng & Yu (2014) the magnetars are produced by newly born isolated fast rotating NSs ($P_i \sim 1$ ms).

In Figure 2, we show the evolutions of accreting NSs with $B_{d,i} = 10^8$ G, while other quantities are kept the same as in Figure 1. The lower initial dipole fields do not change the result qualitatively. In order to trigger r -mode and amplify the toroidal magnetic field within 1 Myr, $s = 0.05$ is required, which is the same as for $B_{d,i} = 10^9$ G. The main difference between $B_{d,i} = 10^8$ G and 10^9 G is in the former case the resultant strengths of B_d and \bar{B}_t are both about three times higher than those obtained in the latter case. This is because r -mode is less suppressed for lower $B_{d,i}$ (see the top panels of Figs. 1 and 2), thus more energy of the mode can be converted into magnetic energy. Anyway, for the accreting NS with $B_{d,i} = 10^8$ G, it could also evolve into a magnetar with $B_d \sim 10^{14}$ G and $\bar{B}_t \sim 10^{16}$ G if its crust is quite elastic. Small s could in fact result in a quite weak damping effect of r -mode,

and thus a small ν_{cr} , which can easily be reached through accretion. In contrast, accreting NSs with large s could finally evolve into MSPs. We suggest that the predecessor of SGR 1745–2900 could be an accreting NS in a special kind of IMXB, in which the NS is orbiting around an evolved companion of $M_c \sim 5.2 M_\odot$ with $P_{\text{orbit}} \simeq 2.53$ d. Moreover, the accreting NS should have a relatively small slippage factor $s (= 0.05)$. Furthermore, accreting NSs with $s > 0.05$ in such IMXBs could finally evolve into MSPs.

4 CONCLUSIONS AND DISCUSSION

We have investigated the evolutions of accreting NSs in a special kind of IMXB, in which the companions are evolved stars in the Hertzsprung gap phase with $M_c \sim 5.2 M_\odot$ and $P_{\text{orbit}} \simeq 2.53$ d. Assuming a duration of 1 Myr for the early Case B RLOF accretion and by adopting a time-averaged rate of $\dot{M} = 6 \times 10^{-8} M_\odot \text{ yr}^{-1}$, the accreting NSs with $P_i = 1.37$ s and $B_{d,i} = 10^8 - 10^9$ G could have their toroidal and dipolar magnetic fields amplified due to r -mode-induced differential rotation and Tayler instability. These accreting NSs could eventually evolve into magnetars with internal toroidal magnetic fields of $\sim 10^{16}$ G and surface dipole magnetic fields of $\sim 10^{14}$ G. The precondition is that they should have quite elastic crusts ($s = 0.05$). We note that the specific evolution process from accreting NSs to magnetars may be more complicated, and more detailed quantitative calculation is still needed. However, our results suggest the magnetic fields of some accreting NSs in a special kind of IMXB could be amplified, and provide a possible explanation for the origin of the GC magnetar SGR 1745–2900. Moreover, accreting NSs with larger s could finally evolve into MSPs. Hence, both magnetars and MSPs could originate from accreting NSs in IMXBs. The high stellar density in the GC should be in favor of forming IMXBs, some of which may further evolve into magnetars and MSPs. We therefore predict more magnetars and MSPs will be observed in the proximity of the GC by future observations.

The relation between magnetars and NS binaries (both HMXBs and low-mass X-ray binaries (LMXBs)) is still an open question and has raised concerns. The possible presence of magnetars in HMXBs has been proposed in many papers (Bozzo et al. 2008; Doroshenko et al. 2010; Reig et al. 2012; Klus et al. 2014; Tsygankov et al. 2016). Moreover, it has been suggested that the soft X-ray source 1E 161348-5055 could be a magnetar in an LMXB (Pizzolato et al. 2008). Our results may also shed light on how magnetars in HMXBs and LMXBs could be formed. Provided that enough angular momen-

um is available through accretion from their companions, the accreting NSs with fairly elastic crusts and relatively small initial spin periods could eventually have their toroidal magnetic fields amplified. The accreting NSs would become magnetars if the enhanced poloidal fields due to Tayler instability could successfully emerge at the NS surfaces, and prevent accreted material from falling on the NS surfaces to avoid field decay. An NS binary comprised of a magnetar and a companion star may finally be formed. Future research will focus on the formation of magnetars in such binaries. Furthermore, in this work we have not considered the interaction between the magnetic fields and the accretion disk, which can exert an additional torque on the NS and affect its spin evolution. The accretion-induced dipole magnetic field decay also has not been taken into account. We will investigate in detail how these effects could affect the evolutions of accreting NSs.

Acknowledgements We thank the anonymous referee, X. D. Li and Y. W. Yu for their helpful comments and suggestions. This work is supported by the National Natural Science Foundation of China (Grant Nos. 11133002 and 11178001).

References

- Alpar, M. A., Cheng, A. F., Ruderman, M. A., & Shaham, J. 1982, *Nature*, 300, 728
- Andersson, N. 1998, *ApJ*, 502, 708
- Bachetti, M., Harrison, F. A., Walton, D. J., et al. 2014, *Nature*, 514, 202
- Bates, S. D., Johnston, S., Lorimer, D. R., et al. 2011, *MNRAS*, 411, 1575
- Bhattacharya, D., & van den Heuvel, E. P. J. 1991, *Phys. Rep.*, 203, 1
- Bonanno, A., & Urpin, V. 2012, *ApJ*, 747, 137
- Bonanno, A., & Urpin, V. 2013a, *ApJ*, 766, 52
- Bonanno, A., & Urpin, V. 2013b, *MNRAS*, 431, 3663
- Bozzo, E., Falanga, M., & Stella, L. 2008, *ApJ*, 683, 1031
- Braithwaite, J. 2006, *A&A*, 453, 687
- Cheng, Q., & Yu, Y.-W. 2014, *ApJ*, 786, L13
- Cuofano, C., & Drago, A. 2010, *Phys. Rev. D*, 82, 084027
- Cuofano, C., Dall’Osso, S., Drago, A., & Stella, L. 2012, *Phys. Rev. D*, 86, 044004
- Cutler, C. 2002, *Phys. Rev. D*, 66, 084025
- Cutler, C., & Jones, D. I. 2001, *Phys. Rev. D*, 63, 024002
- Dai, Z. G., & Lu, T. 1998, *Physical Review Letters*, 81, 4301
- Dall’Osso, S., Perna, R., & Stella, L. 2015, *MNRAS*, 449, 2144
- Dall’Osso, S., Stratta, G., Guetta, D., et al. 2011, *A&A*, 526, A121
- Deneva, J. S., Cordes, J. M., & Lazio, T. J. W. 2009, *ApJ*, 702, L177

- Dexter, J., & O’Leary, R. M. 2014, *ApJ*, 783, L7
- Doroshenko, V., Santangelo, A., Suleimanov, V., et al. 2010, *A&A*, 515, A10
- Eatough, R. P., Falcke, H., Karuppusamy, R., et al. 2013, *Nature*, 501, 391
- Fan, Y.-Z., & Xu, D. 2006, *MNRAS*, 372, L19
- Friedman, J. L., & Morsink, S. M. 1998, *ApJ*, 502, 714
- Fuller, J., & Ott, C. D. 2015, *MNRAS*, 450, L71
- Goldreich, P., & Reisenegger, A. 1992, *ApJ*, 395, 250
- Habets, G. M. H. J., & Heintze, J. R. W. 1981, *A&AS*, 46, 193
- Haskell, B., Degenaar, N., & Ho, W. C. G. 2012, *MNRAS*, 424, 93
- Hessels, J. W. T., Ransom, S. M., Stairs, I. H., et al. 2006, *Science*, 311, 1901
- Ivanova, N., Heinke, C. O., Rasio, F. A., Belczynski, K., & Fregeau, J. M. 2008, *MNRAS*, 386, 553
- Johnston, S., Walker, M. A., van Kerkwijk, M. H., Lyne, A. G., & D’Amico, N. 1995, *MNRAS*, 274, L43
- Johnston, S., Kramer, M., Lorimer, D. R., et al. 2006, *MNRAS*, 373, L6
- Karino, S., & Miller, J. C. 2016, *MNRAS*, 462, 3476
- Kasen, D., & Bildsten, L. 2010, *ApJ*, 717, 245
- Kaspi, V. M., Archibald, R. F., Bhalerao, V., et al. 2014, *ApJ*, 786, 84
- Kennea, J. A., Burrows, D. N., Kouveliotou, C., et al. 2013, *ApJ*, 770, L24
- King, A. R., & Ritter, H. 1999, *MNRAS*, 309, 253
- Klus, H., Ho, W. C. G., Coe, M. J., Corbet, R. H. D., & Townsend, L. J. 2014, *MNRAS*, 437, 3863
- Kluźniak, W., & Lasota, J.-P. 2015, *MNRAS*, 448, L43
- Levin, Y., & Ushomirsky, G. 2001, *MNRAS*, 324, 917
- Lindblom, L., Owen, B. J., & Ushomirsky, G. 2000, *Phys. Rev. D*, 62, 084030
- Lü, H.-J., Zhang, B., Lei, W.-H., Li, Y., & Lasky, P. D. 2015, *ApJ*, 805, 89
- Macquart, J.-P., & Kanekar, N. 2015, *ApJ*, 805, 172
- Macquart, J.-P., Kanekar, N., Frail, D. A., & Ransom, S. M. 2010, *ApJ*, 715, 939
- Mori, K., Gotthelf, E. V., Zhang, S., et al. 2013, *ApJ*, 770, L23
- Olausen, S. A., & Kaspi, V. M. 2014, *ApJS*, 212, 6
- Pan, Y. Y., Wang, N., & Zhang, C. M. 2013, *Ap&SS*, 346, 119
- Pfahl, E., & Loeb, A. 2004, *ApJ*, 615, 253
- Pizzolato, F., Colpi, M., De Luca, A., Mereghetti, S., & Tiengo, A. 2008, *ApJ*, 681, 530
- Rea, N., Israel, G. L., Esposito, P., et al. 2012, *ApJ*, 754, 27
- Rea, N., Esposito, P., Pons, J. A., et al. 2013a, *ApJ*, 775, L34
- Rea, N., Esposito, P., Israel, G. L., et al. 2013b, *The Astronomer’s Telegram*, 5032
- Rea, N., Israel, G. L., Pons, J. A., et al. 2013c, *ApJ*, 770, 65
- Reig, P., Torrejón, J. M., & Blay, P. 2012, *MNRAS*, 425, 595
- Rezzolla, L., Lamb, F. K., & Shapiro, S. L. 2000, *ApJ*, 531, L139
- Rowlinson, A., O’Brien, P. T., Metzger, B. D., Tanvir, N. R., & Levan, A. J. 2013, *MNRAS*, 430, 1061
- Sá, P. M., & Tomé, B. 2005, *Phys. Rev. D*, 71, 044007
- Scholz, P., Kaspi, V. M., & Cumming, A. 2014, *ApJ*, 786, 62
- Shannon, R. M., & Johnston, S. 2013, *MNRAS*, 435, L29
- Shao, Y., & Li, X.-D. 2012, *ApJ*, 756, 85
- Shao, Y., & Li, X.-D. 2015, *ApJ*, 802, 131
- Sigurdsson, S., & Phinney, E. S. 1995, *ApJS*, 99, 609
- Spitler, L. G., Lee, K. J., Eatough, R. P., et al. 2014, *ApJ*, 780, L3
- Tauris, T. M., van den Heuvel, E. P. J., & Savonije, G. J. 2000, *ApJ*, 530, L93
- Thompson, C., & Duncan, R. C. 1995, *MNRAS*, 275, 255
- Thompson, C., & Duncan, R. C. 1996, *ApJ*, 473, 322
- Tsygankov, S. S., Mushtukov, A. A., Suleimanov, V. F., & Poutanen, J. 2016, *MNRAS*, 457, 1101
- Turolla, R., Zane, S., Pons, J. A., Esposito, P., & Rea, N. 2011, *ApJ*, 740, 105
- Urpin, V., Kononkov, D., & Geppert, U. 1998, *MNRAS*, 299, 73
- Verbunt, F., & Freire, P. C. C. 2014, *A&A*, 561, A11
- Yu, Y.-W., Cao, X.-F., & Zheng, X.-P. 2009, *RAA (Research in Astronomy and Astrophysics)*, 9, 1024
- Yu, Y.-W., Cheng, K. S., & Cao, X.-F. 2010, *ApJ*, 715, 477
- Yu, Y.-W., Zhang, B., & Gao, H. 2013, *ApJ*, 776, L40
- Zhang, B., & Mészáros, P. 2001, *ApJ*, 552, L35
- Zhang, C. M., & Kojima, Y. 2006, *MNRAS*, 366, 137